Journal of
Materials Chemistry A

Accepted Manuscript

This article can be cited before page numbers have been issued, to do this please use: M. Zhang, L. Zhang, M. Zhu, Y. Wang, N. Li, Z. Zhang, Q. Chen, L. An, Y. Lin and C. Nan, *J. Mater. Chem. A*, 2016, DOI: 10.1039/C5TA09949H.

This is an *Accepted Manuscript*, which has been through the Royal Society of Chemistry peer review process and has been accepted for publication.

Accepted Manuscripts are published online shortly after acceptance, before technical editing, formatting and proof reading. Using this free service, authors can make their results available to the community, in citable form, before we publish the edited article. We will replace this *Accepted Manuscript* with the edited and formatted *Advance Article* as soon as it is available.

You can find more information about *Accepted Manuscripts* in the Information for Authors.

Please note that technical editing may introduce minor changes to the text and/or graphics, which may alter content. The journal's standard Terms & Conditions and the Ethical guidelines still apply. In no event shall the Royal Society of Chemistry be held responsible for any errors or omissions in this *Accepted Manuscript* or any consequences arising from the use of any information it contains.

ROYAL SOCIETY OF CHEMISTRY

www.rsc.org/materialsA

View Article Online
DOI: 10.1039/C5TA09949H

Journal of Materials Chemistry A

ARTICLE

Controlled Functionalization of Poly(4-methyl-1-pentene) Films for High Energy Storage Applications

Received 00th January 20xx,
Accepted 00th January 20xx

DOI: 10.1039/x0xx00000x

www.rsc.org/

Min Zhang,[a] Lin Zhang,*[b] Meng Zhu,[c] Yiguang Wang,*[c] Nanwen Li,[d] Zhijie Zhang,[e] Quan Chen,[e] Linan An,[f] Yuanhua Lin*[g] and Cewen Nan [g]

A new family of poly(4-methyl-1-pentene) ionomers [PMP-$(NH_3)_x$A-y] (x = 1, 2, 3 and A = Cl^-, SO_4^{2-}, PO_4^{3-}, y = NH_3 content) modified $(NH_3^+)_xA^{x-}$ ionic groups has been synthesized. The ionomers were synthesised using either a traditional Ziegler-Natta or a metallocene catalyst for the copolymerisation of 4-methyl-1-pentene and bis(trimethylsilyl)amino-1-hexene. A systematic study was conducted on the effect of the subsequent work-up procedures that can prevent undesirable side reactions during the synthesis of the [PMP-$(NH_3)_x$A-y] ionomers. The resulting PMP-based copolymers were carefully monitored by a combination of nuclear magnetic resonance (NMR), gel permeation chromatography (GPC), differential scanning calorimetry (DSC), mechanical property, dielectric properties, and electric displacement-electric field (*D*-*E*) hysteresis loop measurements. Our results reveal that the [PMP-$(NH_3)_x$A-y] ionomer films show a significantly enhanced dielectric constant (~5) and higher breakdown field (~ 612 MV/m) as compared with pure PMP films. Additionally, these PMP-based films show good frequency and temperature stabilities (up to 160 °C). A reliable energy storage capacity above 7 J/cm^3 can be obtained, and is twice the energy storage capacity of state-of-the-art biaxially oriented polypropylene films, which can be attractive for technological applications for the energy storage devices.

Introduction

Dielectric materials with a high electric energy density and a low dielectric loss play a very important role in modern electrical power systems, e.g., hybrid electric vehicles, medical defibrillators, filters and switched-mode power supplies.[1–5] Compared to batteries and supercapacitors, dielectric capacitors offer many unique advantages, e.g., fast charge and discharge characteristics, a high power density, a high output voltage, and a wide operating temperature range.[6–11] Compared to other dielectric capacitors, polymer film capacitors are more attractive for the applications mentioned above due to their higher breakdown strength and a more graceful failure mechanism.[3,12,13] In addition, the development of dielectric-polymer-based capacitors has been motivated by the increasing demand for compact, low-cost, light-weight and flexible energy storage devices, which makes polymer films the material of choice for the next generation of high pulse capacitors.[14,15] However, polymer film capacitors generally suffer from either a low dielectric constant or an unacceptably large energy loss.[3,16–19] For example, although biaxially oriented polypropylene (BOPP) exhibits a high breakdown strength (E_b > 600 MV/m) and an inherently low energy loss (tan δ ~ 0.0002), BOPP-based thin film capacitors can only offer an energy density in the range from 2 to 3 J/cm^3 at E_b = 600 MV/m due to the material's low dielectric constant (ε_r = 2.2).

In general, the energy density U_e of a dielectric is defined as:

$$U_e = \int E \cdot dD \qquad (1)$$

where E is the applied electric field and D is the electric displacement. Therefore, a high U_e can not only be achieved by increasing E but also by increasing D. In the past few decades, poly(vinylidene fluoride) (PVDF)-based ferroelectric polymers have attracted much attention because of their relatively high displacement (~10 μC/cm^2).[20–29] As a result of strong C–F dipoles and the spontaneous orientation of dipoles in the crystalline phases, such ferroelectric polymers possess a higher dielectric constant (12–15 at 1 kHz) at room temperature than other known polymers.[20,30,31] It was demonstrated that the incorporation of bulky monomers such as chlorotrifluoroethylene (CTFE) and hexafluoropropylene (HFP) into the PVDF main chain yields slimmer polarization loops and higher discharge energy densities (U_e > 25 J/cm^3) at high electric fields (> 600 MV/m).[4,22,24] Utilizing PVDF-based copolymers as a representative uniaxially stretched ferroelectric polymer material, the energy density could be improved by an order of magnitude compared to BOPP.[4] Unfortunately, the presence of highly coupled dipole interactions and large ferroelectric domains in the ferroelectric polymers results

[a] College of Materials Science and Engineering, Beijing Institute of Petrochemical Technology, Beijing, 102617, China.
[b] Materials Research and Education Center, Auburn University, Auburn, AL 36849, USA. Email: lzz0002@auburn.edu.
[c] State Key Laboratory of Solidification Processing, Northwestern Polytechnical University, Xi'an, 710072, China. Email: wangyiguang@nwpu.edu.cn.
[d] State Key Laboratory of Coal Conversion, Institute of Coal Chemistry, Chinese Academy of Science, Taiyuan, 030001, China.
[e] State Key Laboratory of Polymer Physics and Chemistry, Changchun Institute of Applied Chemistry, Chinese Academy of Sciences, Changchun, 130022, China.
[f] Department of Materials Science and Engineering, Advanced Materials Processing and Analysis Center, University of Central Florida, Orlando, FL 32816, USA.
[g] School of Materials Science and Engineering, State Key Lab of New Ceramics and Fine Processing, Tsinghua University, Beijing 100084, China. Email: linyh@mail.tsinghua.edu.cn.

Electronic Supplementary Information (ESI) available: [details of any supplementary information available should be included here]. See DOI: 10.1039/x0xx00000x

View Article Online
DOI: 10.1039/C5TA09949H

in a high energy barrier for a switch of the dipole direction and a strong polarization hysteresis, which in turn leads to a high dielectric loss.[32–34]

Recently, the grafting of polystyrene or poly(methacrylate ether) side chains onto PVDF copolymers has been reported to result in the formation of insulating layers around the polar crystal domains, which significantly decreased the dielectric constant and loss and increased E_b. Eventually, energy densities of up to 17.5 J/cm^3 could be achieved.[35–39] Recently, Wang *et al*.[40] proposed a simple and scalable cross-linking method for the synthesis of cross-linked PVDF, which resulted in a higher dielectric constant, a lower dielectric and conductive loss, and a higher breakdown strength. Nevertheless, experimental results showed that these modifications to PVDF-based copolymers and terpolymers cannot fully suppress the polarization coupling in these ferroelectric polymers, especially at high electric fields (> 10 MV/m) Therefore, some research groups have turned to linear dielectrics. For linear dielectrics, the energy density can be expressed as:

$$U_e = 1/2\varepsilon_0\varepsilon_r E^2 \qquad (2)$$

where ε_0 is the vacuum permittivity (8.85×10^{-12} F/m) and ε_r is the relative dielectric constant. Compared with ferroelectric polymers, the dielectric properties of non-ferroelectric polymers are more stable over a large frequency and temperature range, and such polymers, e.g., poly(ether ether ketone) (PEEK), poly(phthalazinone ether ketone) (PPEK), and polypropylene with polar side groups (PP-OH copolymers) exhibit a very low dielectric loss and higher breakdown strengths.[41–44] For example, Zhang *et al*.[45,46] reported on the synthesis of an amorphous and glass phase aromatic polythiourea with a high breakdown strength of up to 1.1 GV/m an energy density above 24 J/cm^3 and a low energy loss below 150 °C. The addition of a small amount (2−6 mol.%) of −OH groups to isotactic polypropylene (PP) can significantly increase the material's dielectric constant while maintaining a relatively low dielectric loss after stretching, which was also confirmed by simulations.[43,44]

Besides increasing the energy density and reducing the energy loss, thermal management is another approach that allows for the application of dielectric polymers at elevated temperatures. The best commercially available dielectric polymer BOPP can only be used at temperatures below 105 °C.[3] Therefore, it is of great interest to study the dielectric properties of novel ion-containing poly(4-methyl-1-pentene) (PMP) copolymers with high melting temperatures above 220 °C. It is believed that ion-containing polymers are not suitable for achieving a high U_e and a high E_b due to the significant conduction loss at a high electric field. However, we believe that E_b is more strongly affected by the quality of the films than the ion-induced conductive loss. Furthermore, ion-containing polymers are more suitable for film stretching due to the enhancement of the melt viscosity caused by the ionic association and the improved mechanical properties.

In this study, a family of poly(4-methyl-1-pentene) copolymers PMP-$(NH_3)_x$A-y containing various $–NH_3^+Cl^–$, $–(NH_3)_2SO_4^{2-}$ and $–(NH_3)_3PO_4^{3-}$ side groups were systematically investigated. These chemically modified PMP polymers were prepared and then fabricated into thin films for comparative dielectric and electric energy storage experiments. The combined effect of the addition of the side-chain groups (comonomer units) and the subsequent thin film fabrication step on the dielectric properties of the resulting polymer films was explored. The modified PMP polymers showed a high energy density (> 7 J/cm^3) at 600 MV/m, a high charge-discharge energy efficiency (> 93%) and could withstand temperatures of up to 160 °C, which makes them attractive for a potential application in high-energy density capacitors.

Experimental Section

Materials

All O_2- and moisture-sensitive manipulations were performed under argon atmosphere in a glovebox. 4-Methyl-1-pentene was purchased from Tokyo Chemical Industry (Shanghai) and distilled over CaH_2 under reduced pressure before use. Triethylaluminium (TEA, 1.3 M in heptane), diethylaluminium chloride ($AlEt_2Cl$, 0.9 M in toluene), aluminium-activated titanium(III) chloride ($TiCl_3$·AA) and calcium hydride were purchased from J&K Scientific Ltd. All other chemicals, including methanol, sodium hydroxide, toluene, hydrochloric acid, sulphuric acid and phosphoric acid were of analytical grade and purchased from Sigma-Aldrich and used as received. Toluene was distilled over a sodium/potassium alloy with benzophenone as indicator under argon atmosphere. 6-Bis(trimethylsilyl)amino-1-hexene was prepared according to a procedure described in literature.[47,48]

Copolymerisation of 4-methyl-1-pentene/bis(trimethylsilyl)amino-1-hexene

For comparison, 4-methyl-1-pentene/bis(trimethylsilyl)amino-1-hexene was synthesised using either a Ziegler-Natta catalyst or a metallocene catalyst. In the first case, in a typical copolymerisation reaction, 50 mL of toluene and 10 mL of 4-methyl-1-pentene were poured into a Parr 450 mL stainless autoclave equipped with a mechanical stirrer in the glovebox. After removal from the glovebox, a certain amount of bis(trimethylsilyl)amino-1-hexene was injected into the reactor, heated and left at a constant temperature of 60 °C under stirring and argon gas protection. Either about 0.2 g of $TiCl_3$·AA and 5.0 mL of $AlEt_2Cl$ or 0.2 g of $TiCl_3$·AA and 5.0 mL of $AlEt_3$ were mixed together and stirred for 30 min in the glovebox at room temperature to activate the catalyst, and then injected into the reactor under rapid stirring to initiate the copolymerisation reaction. After 30 min at 60 °C, the reaction solution was quenched with tetrahydrofuran (THF), filtered and extensively washed with THF to remove residual monomers. The isolated 4-methyl-1-pentene/bis(trimethylsilyl)amino-1-hexene copolymer was dried under vacuum at room temperature for 12 h. Alternatively, the reaction solution was directly quenched with a methanolic hydrogen chloride solution to convert the incorporated $–N(SiMe_3)_2$ groups to the stable $–NH_3^+Cl^–$ groups. In the second case, when using a metallocene catalyst, a similar procedure was used, except that the catalyst system was changed to *rac*-$Me_2Si[2\text{-}Me\text{-}4\text{-}Ph(Ind)]_2ZrCl_2$ (5×10^{-6} M) and d-MAO (0.35 g, Al/Zr = 1000). The reaction temperature was 25 °C and the reaction time was 60 min. After the reaction, the products were washed with THF and methanol three times before drying.

Conversion of the bis(trimethylsilyl)-amine groups into functional groups

The bis(trimethylsilyl)-amine ($–N(SiMe_3)_2$) groups in the poly(4-methyl-1-pentene) (PMP) copolymers were further converted to the desired $–NH_3^+Cl^–$ and $–NH_2$ groups. To this end, about 3 g of the 4-methyl-1-pentene/bis(trimethylsilyl)amino-1-hexene copolymer was suspended in 50 mL THF at 50 °C. Then, 20 ml of a 2 M methanolic hydrogen chloride solution was added dropwise. The

View Article Online
DOI: 10.1039/C5TA09949H

mixture was stirred for 4 h at 50 °C, and the resulting PMP-$NH_3^+Cl^-$ polymer was collected by filtration and washed with deionized water several times before drying at 60 °C in vacuum for 24 h. For the preparation of the PMP-NH_2 polymer, after the deprotection reaction with the methanolic hydrogen chloride solution, the polymer solution was poured into 100 ml of a 1 M methanolic NaOH solution. The resulting polymer was collected by filtration and washed with a 1 M aqueous ammonia solution and water under nitrogen atmosphere. After drying at 50 °C in vacuum overnight, the resulting PMP-NH_2 copolymer was obtained with quantitative yield. The amino group reactions also occur in the polymer film. Thus, the PMP-NH_2 copolymer can be moulded into a film first, and then converted into PMP-$NH_3^+Cl^-$, PMP-$(NH_3)_2SO_4^{2-}$ or PMP-$(NH_3)_3PO_4^{3-}$ films by submerging the PMP-NH_2 film into a 2 M methanolic hydrogen chloride solution, a 2 M methanolic sulphuric acid solution or a 2 M methanolic phosphoric acid solution, respectively.

Film fabrication and processing

The PMP-NH_2-y films were prepared by hot pressing in vacuum at 240 °C and at a pressure of 24.000 psi to remove defects, resulting in an average film thickness in the range from 40 to 50 µm. These films were placed in beakers, and then a 2 M methanolic hydrogen chloride solution, a 2 M methanolic sulfuric acid solution or a 2 M methanolic phosphoric acid solution was added under stirring to obtain the corresponding PMP-$NH_3^+Cl^-$-y, PMP-$(NH_3)_2SO_4^{2-}$-y or PMP-$(NH_3)_3PO_4^{3-}$-y polymer films, respectively. After completion of the reactions, the films were washed with deionized water to remove excess acid and then dried overnight at 60 °C, followed by another drying step in vacuum at 70 °C for 8 h. The stretched films were eventually produced by uniaxially stretching the obtained films at 130 °C and at an extension rate of 10mm·min^{-1} to an extension ratio of about 600%, resulting in a final thickness of approx. 11 µm.

Sample characterization

All high-temperature ^1H NMR spectra were recorded on a Bruker AM-300 nuclear magnetic resonance (NMR) spectrometer in a 1,1,2,2-tetrachloroethane-d_2 atmosphere at 110 °C. The polymer molecular weights were measured by gel permeation chromatography (GPC) on a PL-GPC 220 High Temperature GPC/SEC System equipped with four PLgel Mixed-A (20 µm) columns. The oven temperature was set to 150 °C and the temperatures of the autosampler's hot and warm zones were 135 and 130 °C, respectively. The solvent 1,2,4-trichlorobenzene (TCB) containing ~200 ppm tris(2,4-di-tert-butylphenyl) phosphite (Irgafos 168) was purged with nitrogen. The flow rate was adjusted to 1.0 mL/min and the injection volume was 200 µL. A test specimen with a concentration of 2 mg/mL was prepared by dissolving the sample in the N_2-purged and preheated TCB (containing 200 ppm Irgafos 168) for 2.5 h at 160 °C with gentle agitation. The melting temperatures of the polymers were obtained by differential scanning calorimetry (DSC) using a Perkin-Elmer DSC-7 instrument controller with a heating rate of 20 °C/min. Fourier transform infrared spectroscopy (FTIR) was performed on a PE-1710 spectrometer in the wavenumber range from 4000 to 400 cm^{-1} with a 4 cm^{-1} resolution. 64 scans were conducted on each of the polymer thin films. Atomic-force microscopy (AFM) micrographs were recorded with a bioatomic force microscopy (Bio-AFM). AFM tapping-mode height profiles were acquired with a JPK Instruments AG multimode NanoWizard (Germany). The instrument was equipped with a NanoWizard scanner. For tapping-mode AFM, a commercial Si cantilever (TESP tip) of 320 kHz resonant frequency from JPK was used. X-ray diffraction (XRD) analysis was carried out with a Bruker D8 advance (Germany). The wavelength of the X-rays was 1.542 Å (Cu Kα radiation, 40 kV and 100 mA), and the scanning rate was 4° min^{-1}. All mechanical properties (tensile strength, tensile modulus, elongation at break, etc.) were measured according to the ASTM D-1708 test method. The dog bone-shaped specimens with an overall size of 38 mm × 15 mm (5 mm × 22 mm in the gauge area) were-die cut, and then the mechanical tests were performed on an Instron 5866 universal testing machine using a load cell of 100 N and a constant cross head speed of 1 mm/min. At least 5 samples of each type were studied in order to minimize possible errors. For the electrical measurements, gold electrodes with a thickness of approx. 80 nm were sputtered onto both surfaces of the film using a JEOL JFC-1600 auto fine coater (Japan). The dielectric properties were then measured using an Agilent (4294A) precision impedance analyser in the frequency range from 100 Hz to 1 MHz at 1 V, and in a temperature range from -20 to 160 °C. The *D-E* hysteresis loops were recorded at room temperature on a Premiere II ferroelectric test system at a frequency of 10 Hz.

Results and discussion

Synthesis and characterization of PMP-$(NH_3)_xA$-y copolymers

As illustrated in **Scheme 1**, the PMP-$N(SiMe_3)_2$-y copolymers were synthesized by copolymerisation of 4-methyl-1-pentene with bis(trimethylsilyl)amino-1-hexene comonomers (Figure S1), using either a homogeneous metallocene catalyst or a heterogeneous Ziegler-Natta catalyst. Recently, Chung *et al.*[47,48] reported on the preparation of amino-functionalized polyolefins from silane-protected α,ω-aminoolefin via a metallocene catalyst-mediated copolymerisation process, which resulted in the formation of random PE-$NH_3^+Cl^-$ and PP-$NH_3^+Cl^-$ ionomers. In contrast, a heterogeneous Ziegler-Natta catalyst is almost incapable of incorporating the bulky α,ω-bis(trimethyl)aminoolefin during propylene copolymerisation probably due to the large difference in both size between the two comonomers and their reactivity ratios. Compared to the highly reactive propylene monomers, 4-methyl-1-pentene may be a more promising candidate for copolymerisation with bis(trimethylsilyl)amino-1-hexene via a Ziegler-Natta catalyst.

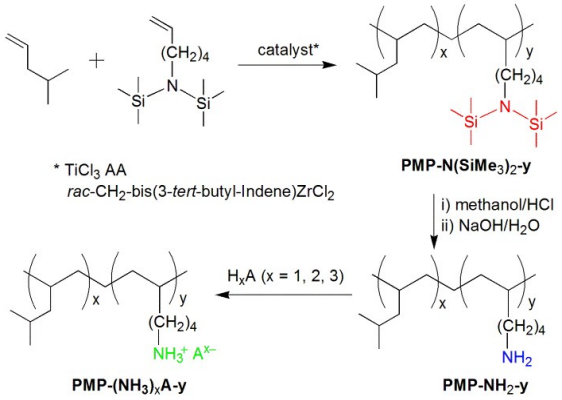

Scheme 1 Illustration of the synthesis of PMP-NH_2-y and PMP-$(NH_3)_xA$-y copolymers (A = Cl^-, SO_4^{2-} or PO_4^{3-}; y = NH_2 content; x = 1, 2, 3) via a catalytic copolymerisation process.

View Article Online
DOI: 10.1039/C5TA09949H

The resulting PMP-N($SiMe_3$)$_2$-y copolymer, with the pendant silane-protected amino groups, can be directly deprotected using a HCl/methanol solution during the sample work-up process to form stable PMP-$NH_3^+Cl^-$-y ionomers, which can be subsequently neutralized with an NaOH aqueous solution under an inert atmosphere to obtain PMP-NH_2-y. The reactive amino groups in the PMP-NH_2-y copolymers can react with various acids, including hydrochloric acid, sulphuric acid and phosphoric acid to synthesise corresponding PMP ionomers, denoted as PMP-$(NH_3)_x$A-y (A = Cl^-, SO_4^{2-} and PO_4^{3-}; x = 1, 2, 3).

Table 1 compares selected properties of the reaction products obtained through two parallel sets of 4-methyl-1-pentene/bis(trimethylsilyl)amino-1-hexene copolymerisation reactions using three different catalyst systems, i.e., the two heterogeneous Ziegler-Natta catalysts $TiCl_3$·AA/Et_2AlCl and $TiCl_3$·AA/Et_3Al and the homogeneous metallocene catalyst *rac*-CH_2-bis(3-*tert*-butyl-indene)$ZrCl_2$/d-MAO. Overall, all copolymerisation reactions produced copolymers with an incorporation ratio in the range from 1.9 to 5.1, indicating that both catalytic systems possess suitable comparative comonomer reactivity. In the Ziegler-Natta catalyst-mediated copolymerisation reactions, it is essential to use the Et_3Al co-catalyst. The use of Et_2AlCl causes an aversive effect in the formation of the completely insoluble PMP-N($SiMe_3$)$_2$-y copolymer. The Et_2AlCl may *in situ* activate $TiCl_3$·AA due to the formation of a trace amount of HCl, which may break the reactive N–Si bonds in the pendent –N($SiMe_3$)$_2$ groups of the PMP-N($SiMe_3$)$_2$-y copolymer, which then engage in an intermolecular dimerization reaction, resulting in the formation of a cross-linked polymer network, according to Chung's report.[47]

Table 1 Comparison of selected properties of the reaction product obtained through the 4-methyl-1-pentene/6-bis(trimethylsilyl)amino-1-hexene copolymerisation for different reaction conditions.

Reaction conditions				Copolymerisation results					
run[a]	co-catalyst	comonomer[b] (mL)	Polymer yield (g)	[comonomer][c] (mol%)	M_w[d] (kg/mol)	PDI[d]	T_g[e] (^{o}C)	T_m[e] (^{o}C)	ΔH[e] (J/g)
A-1	Et_2AlCl	0	3.8	0	204	5.35	51.2	234.8	59.8
A-2	Et_2AlCl	0.5	2.7	–	–	–	33.2	223.4	51.4
A-3	Et_3Al	0	3.5	0	211	5.67	52.3	235.3	60.1
A-4	Et_3Al	0.5	2.9	1.9	189	6.06	31.3	224.9	49.3
A-5	Et_3Al	1.0	2.5	3.1	168	5.88	30.8	224.5	48.9
A-6	Et_3Al	2.0	1.9	4.5	159	5.95	30.5	224.1	48.4
B-1	dMAO	0	4.7	0	210	2.34	–	156.8	110.2
B-2	dMAO	0.5	3.6	2.4	166	2.18	–	–	–
B-3	dMAO	1.0	2.7	5.1	154	2.45	–	–	–

[a]Catalyst used in set A: $TiCl_3$·AA (reaction temperature: 60 °C, reaction time: 30 min); set B: *rac*-CH_2-bis(3-*tert*-butyl-indene)$ZrCl_2$ (reaction temperature: 25 °C, reaction time: 60 min). [b]10 mL of 4-methyl-1-pentene and 6-bis(trimethylsilyl)amino-1-hexene added as comonomer. [c] Comonomer content (mol.%) in the copolymers as determined by ^{1}H NMR spectroscopy at 110 °C in 1,1,2,2-tetrachloroethane-d_2. [d]The weight-average molecular weights and the polydispersity index were determined by GPC at 150 °C in 1,2,4-trichlorobenzene vs. narrow polystyrene standards. [d] Determined by DSC.

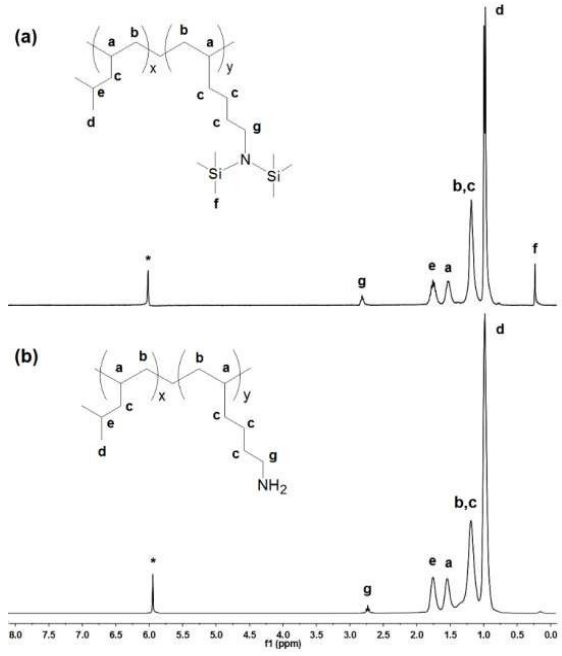

Fig. 1 ^{1}H NMR spectra obtained for (a) PMP-N($SiMe_3$)$_2$-4.5 and (b) PMP-NH_2-4.5 in 1,1,2,2-tetrachloroethane-d_2 at 110 °C.

When using the traditional Ziegler-Natta catalyst $TiCl_3$·AA/Et_3Al, soluble PMP copolymers with a high molecular weight (M_w > 145 kg/mol), a typical molecular weight distribution (4.68–6.55) and > 4 mol% –N($SiMe_3$)$_2$ comonomer units are produced, which is sufficient to investigate the effect of different NH_2-transferred ionomer groups on the dielectric and capacitor properties, as shown in Figure S2. Unfortunately, the homogeneous metallocene system produces amorphous PMP copolymers with a higher comonomer content and a narrower molecular weight distribution (Figure S3), which is not ideal for a potential application in capacitors due to the poor mechanical properties, which are not suitable for the film pressing and the subsequent film stretching process. In particular, for the PMP-N($SiMe_3$)$_2$-y copolymers obtained using the $TiCl_3$·AA/Et_3Al Ziegler-Natta catalyst, both the T_m and ΔH_m values show an initial reduction and then subsequently level off at a

View Article Online
DOI: 10.1039/C5TA09949H

higher comonomer content, as shown in Table 1 and Figure S4, which is similar to results previously reported in literature.[43]

The ^{1}H NMR spectra of a typical pair of PMP copolymers before and after the silane group deprotection reaction is shown Figure 1. The combination of the complete disappearance of the sharp N–Si–$(CH_3)_3$ peak at 0.21 ppm and the coexistence of a $–CH_2–NH_2$ peak at 2.77 ppm indicates a successful deprotection. The NH_2 group content in the copolymer was determined by relating the peak intensity to the number of protons in the N–Si–$(CH_3)_3$ group of the copolymer or the $CH_2–NH_2$ group of the copolymer. In Figure S5, two absorption peaks at around 3400 and 1640 cm^{-1}, which indicate the presence of amine groups in PMP-NH_2.

The optimal way to investigate a copolymerisation reaction is to measure the reactivity ratio of the comonomers. To obtain meaningful results, a series of experiments were conducted by varying the monomer feed ratio (ρ = [4-methyl-1-pentene]/[bis(trimethylsilyl)amino-1-hexene] = $[M_1]/[M_2]$) and comparing the resulting copolymer composition (R = $d[M_1]/d[M_2]$) at a low monomer conversion (< 5%) required to maintain a constant comonomer mole ratio ($[M_1]/[M_2]$). In the Supporting Information, Tables S1 and S2 summarize the results of two sets of experiments of 4-methyl-1-pentene/bis(trimethylsilyl)amino-1-hexene copolymerisation that were conducted using either a heterogeneous $TiCl_3$·AA/Et_3Al Ziegler-Natta catalyst or a homogeneous *rac*-Me_2Si[2-Me-4-Ph(Ind)]$_2ZrCl_2$/dMAO metallocene catalyst, respectively. The reactivity ratios for 4-methyl-1-pentene ($r_1 = k_{11}/k_{12}$) and bis(trimethylsilyl)amino-1-hexene ($r_2 = k_{22}/k_{21}$) were estimated using the Fineman-Ross equation. Both plots in Figure S6 yield straight lines with slope r_1 and intercept r_2. For the linear slope in Figure S6 (a), r_1 = 2.09 and r_2 = 0.11, with $r_1 \times r_2$ = 0.23 (not far from unity), indicating a relatively good random copolymerisation reaction with a slightly higher 4-methyl-1-pentene reactivity in the *rac*-Me_2Si[2-Me-4-Ph(Ind)]$_2ZrCl_2$/dMAO-mediated homogenous 4-methyl-1-pentene/bis(trimethylsilyl)amino-1-hexene copolymerisation reactions. In other words, the 4-methyl-1-pentene/bis(trimethylsilyl)amino-1-hexene copolymers obtained in runs B1–B3 (Table 1) are mostly random copolymers. As discussed later, they also showed a narrow molecular weight distribution. On the other hand, the similar linear 4-methyl-1-pentene/bis(trimethylsilyl)amino-1-hexene copolymerisation plot in Figure S6 (b) yields r_1 = 4.14 and r_2 = 0.34 with $r_1 \times r_2$ = 1.41 (not far from unity), indicating a strong tendency of a consecutive 4-methyl-1-pentene insertion when using a heterogeneous Ziegler-Natta catalyst system ($TiCl_3$·AA/Et_3Al). Meanwhile, due to the much higher 4-methyl-1-pentene reactivity in the copolymerisation reactions observed for the runs A1-6 (Table 1), the PMP-N($SiMe_3$)$_2$-y copolymers showed a tapered molecular structure with incorporated side-chain units concentrated at one end of the copolymer main chain. Therefore, an increase of the comonomer content has little effect on the PMP chain crystallization, which is consistent with the DSC results presented in Table 1. Similar results were also reported for PP-OH copolymers.[43]

It is interesting to note that all samples prepared by Ziegler-Natta catalyst, including PMP homopolymer, copolymer with 4.5 mol% NH_2-comonomer units and PMP-based ionomers (PMP-NH_3Cl-4.5, PMP-$(NH_3)_2SO_4^{2-}$-4.5 and PMP-$(NH_3)_3PO_4^{3-}$-4.5) exhibit sharp XRD peaks and maintain semicrystalline (Figure S7). The introduction of 4.5 mol% NH_2-containing side chains into PMP backbone leads to weaker XRD peaks compared to PMP homopolymer due to the disruption of crystallinity by incorporated short side chains located in amorphous phase. Of particular, it's expected that PMP-NH_2-4.5 shows sharper XRD peak (higher crystallinity) than those of PMP-based ionomers, which can be ascribed to the fact that the incorporation of ion-pairs into polymer short side chains may absorb water and swell to increase amorphous contents, with crystalline phase keeping intact.

Mechanical properties of PMP-$(NH_3)_x$A-y copolymers

The effect of ionic association (physical cross-linking) on the mechanical properties of the PMP copolymers is investigated, and AFM observations for the microstructure of PMP-based ionomer membranes were performed and shown in Figure S8. As shown in Figure S8, the dark areas represent hydrophilic (ionic) domains, and the brighter areas represent hydrophobic domains. The phase surface image exhibits hydrophilic–hydrophobic phase separation, spreading as sea-islands structure, with small ionic domains size ranging from 5–60 nm for PMP-$NH_3^+Cl^-$-4.5. As to PMP-$(NH_3)_2SO_4^{2-}$-4.5, the phase surface image becomes not average as that of PMP-$NH_3^+Cl^-$-4.5, probably due to physical cross-linking effect by SO_4^{2-} groups. In addition, PMP-$(NH_3)_3PO_4^{3-}$-4.5 shows not so clear phase separation compared to those of PMP-$NH_3^+Cl^-$-4.5 and PMP-$(NH_3)_2SO_4^{2-}$-4.5, mainly due to stronger cross-linking. Table 2 summarizes the results of the tensile strength, tensile modulus and elongation at break (%) measurements performed at 25 °C. All specimens were prepared and tested under identical operating conditions, and the measurements were repeated several times to obtain the average values and the ranges of deviation. The PMP-$NH_3^+Cl^-$-4.5 ionomer showed a lower tensile strength and a lower Young's modulus but was more ductile with a higher elongation at break compared to the pure PMP homopolymer. In contrast, the PMP-$(NH_3)_3$-PO_4^{3-}-4.5 ionomer exhibited a remarkably improved tensile strength and Young's modulus as well as a higher elongation at break in comparison with the pure PMP film.

Table 2 Summary of mechanical properties of the PMP ionomers

Sample	Tensile strength (MPa)	Young's modulus (MPa)	Elongation at break (%)
PMP	25±5	1155±105	28±6
PMP-NH_2-4.5	15±2	895±45	45±9
PMP-Cl^--4.5	13.8±1.6	775±35	58±7
PMP-SO_4^{2-}-4.5	23.8±0.8	1048±45	53±9
PMP-PO_4^{3-}-4.5	26.5±1.5	1215±55	38±6

Dielectric response under low electric fields

Figure 2 systematically compares the dielectric constant (ε_r) and dielectric loss (tan δ) profiles obtained for pure PMP and three different PMP-$NH_3^+Cl^-$-y ionomers containing 1.9 (run A-4), 3.1 (run A-5) and 4.5 mol% (run A-6) $NH_3^+Cl^-$ comonomer units, respectively, recorded over a frequency range from 100 to 1 MHz at room temperature. The dielectric constant of the pure PMP polymer film is around 2.15, accompanied by a low dielectric loss of 3×10^{-4}, both of which are frequency independent.

View Article Online
DOI: 10.1039/C5TA09949H

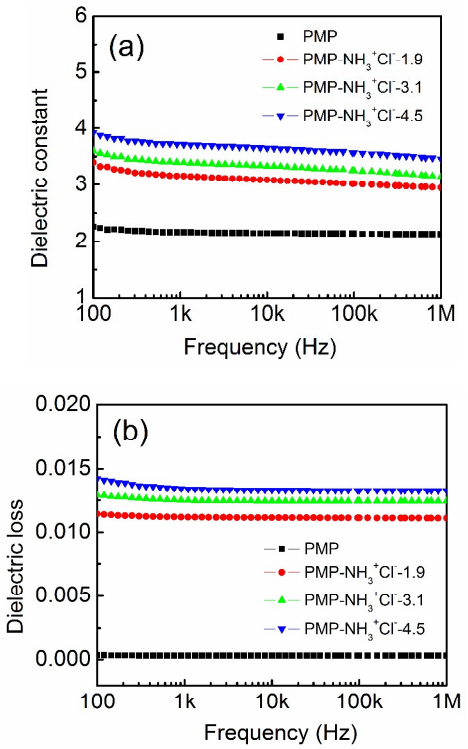

Fig. 2 Frequency dependence at room temperature of (a) the dielectric constant and (b) the dielectric loss of PMP for different amounts of Cl^-.

The dielectric constant increases proportionally with the $NH_3^+Cl^-$ content, reaching 3.8 for PMP- $NH_3^+Cl^-$-4.5 (Figure 2(a)), which was accompanied by a higher frequency dependency. The increase in ε_r is probably due to the strong ionic polarization of the $NH_3^+Cl^-$ functional groups and a much weaker electron polarization along the direction of the applied electric field. At high frequencies, the relatively slow segmental motion of the polymer chains is significantly inhibited, and therefore ε_r monotonically decreases with the frequency. In Figure 2(b), the dielectric loss increases from 3×10^{-4} to 0.014 for the PMP-based polymers due to the loss in electric conductivity caused by the incorporation of the $NH_3^+Cl^-$ groups. However, the dielectric loss obtained for PMP-$NH_3^+Cl^-$-4.5 is still much lower than the dielectric loss of many known dielectric polymers, e.g., PVDF.[40]

The weak-field dielectric properties of the PMP-$(NH_3)_x$A-4.5 ionomers with different anion groups A, i.e., Cl^-, SO_4^{2-} and PO_4^{3-}, were characterized as a function of the frequency. As shown in Figure 3(a), the ε_r value observed for PMP-$(NH_3)_3PO_4^{3-}$-4.5 was as high as 5.1 (more than twice the ε_r of PP), which is slightly higher than the values obtained for PMP-$NH_3^+Cl^-$-4.5 and PMP-$(NH_3)_2SO_4^{2-}$-4.5 with the same NH_3^+-containing comonomer content, especially in the high frequency range, probably due to the fact that the PO_4^{3-} ion has more negative charges and therefore a stronger ionic polarization. Furthermore, the dielectric constant of the PMP-$(NH_3)_3PO_4^{3-}$-4.5 polymer film is less dependent on the frequency compared with the PMP-$NH_3^+Cl^-$-4.5 and PMP-$(NH_3)_2SO_4^{2-}$-4.5 polymer films. Figure 3(b) illustrates the frequency dependence of the dielectric loss for PMP-$NH_3^+Cl^-$-4.5, PMP-$(NH_3)_2SO_4^{2-}$-4.5 and PMP-$(NH_3)_3PO_4^{3-}$-4.5. A surprisingly low dielectric loss of 0.0081 was observed for PMP-$(NH_3)_3PO_4^{3-}$-4.5 compared to PMP-$NH_3^+Cl^-$-4.5 and PMP-$(NH_3)_2SO_4^{2-}$-4.5. The AC conductivity was calculated from dielectric properties which are shown in Figure S9 according to literatures[49–51]. The conductivity of PMP PMP-$(NH_3)_x$A-4.5 ionomers with different anion groups is smaller than 10^{-5} S/m from 100 Hz to 1 MHz and shows a linear relationship with frequency. It indicates that these polymers show good dielectric properties with very low conductivity.

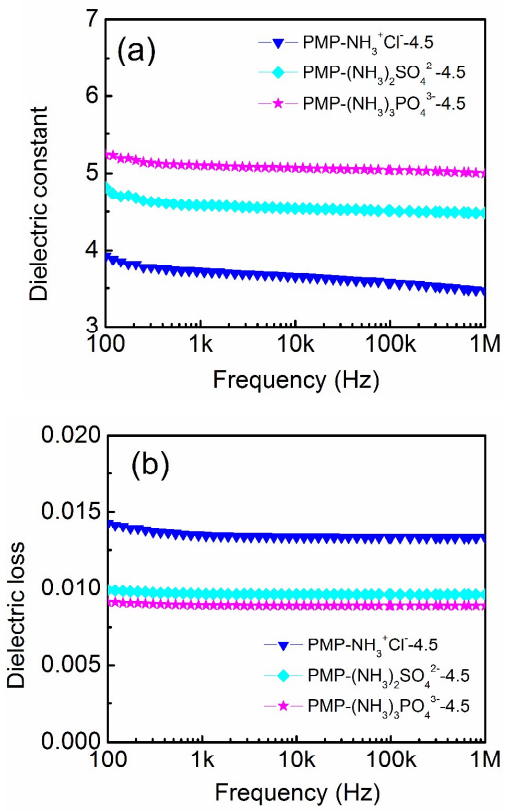

Fig. 3 Frequency dependence of (a) the dielectric constant and (b) the dielectric loss of PMP-NH3+Cl^--4.5, PMP-$(NH3)_2SO_4^{2-}$-4.5 and PMP-$(NH3)_3PO_4^{3-}$-4.5 at room temperature.

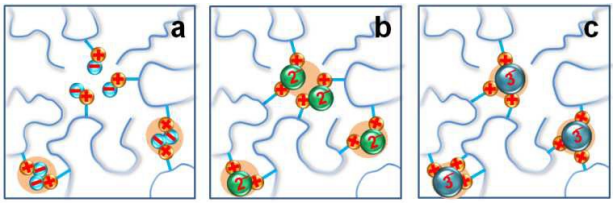

Scheme 2 Ionic association in PMP: (a) Cl^-, (b) SO_4^{2-}, and (c) PO_4^{3-}.

The improved dielectric properties of PMP-$(NH_3)_3PO_4^{3-}$-4.5 are attributed to the ionic association mechanism illustrated in Scheme 2. For PMP-$NH_3^+Cl^-$-4.5, because Cl^- only has one negative charge, there is a high probability that the Cl^- ion cannot connect with

View Article Online
DOI: 10.1039/C5TA09949H

another positive charge carrier located on the inter- or intra-polymer chain, and, as a result, is just randomly distributed in the polymer matrix based on the polymer phase separation mechanism. In contrast, the bulkier and heavier PO_4^{3-} with three negative charges requires three NH_3^+ ions to form saturated and stable ion-pairs, which helps to build a stronger network structure resulting in a better segment stability (immobility and reversibility), and therefore the ionomer exhibits a lower dielectric loss under an applied electric field in the frequency range from 100 Hz to 1 MHz. These results are in good agreement with the results of the mechanical property measurements listed in Table 2.

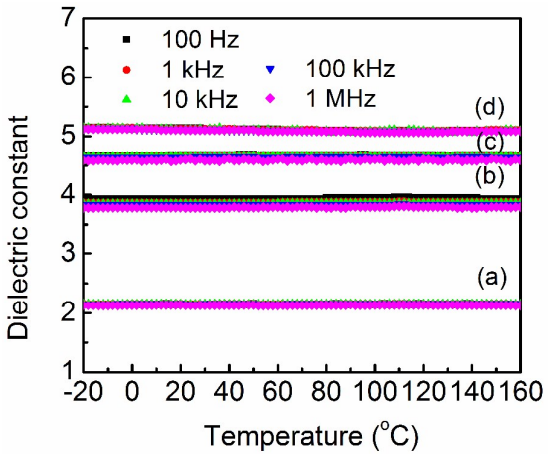

Fig. 4 Temperature dependence of the dielectric constant for (a) PMP, (b) PMP-$NH_3^+Cl^-$-4.5, (c) PMP-$(NH_3)_2SO_4^{2-}$-4.5, and (d) PMP-$(NH_3)_3PO_4^{3-}$-4.5 in the temperature range from -20 to 160 °C.

The temperature dependence of dielectric constants of pure PMP polymer and the PMP ionomers samples over a temperature range from -20 to 160 °C is shown in Figure 4 The selected frequencies care from 100 Hz to 1 MHz. The dielectric profiles recorded for all of the PMP-based ionomers resemble the PMP profile, with the dielectric constant not depending on the temperature. The curves almost overlap and are rather flat at room temperature, which is not only in good agreement with the results shown in Figure 2 and Figure 3, but also indicates a fast polarization response for the PMP copolymers in the temperature range from –20 to 160 °C. In fact, most of the current polymer-based capacitors, e.g., BOPP, can only be operated at temperatures below 105 °C due to the significant change of the material's dielectric and mechanical properties at higher temperatures. For PMP-$(NH_3)_3PO_4^{3-}$-4.5, the dielectric constant was found to be considerably stable with respect to the temperature for temperatures up to 160 °C, which indicates that this class of polymers is a promising candidate for high-temperature capacitor applications. Meanwhile, the dielectric constants showed no abrupt peaks at the glass transition temperatures of the corresponding polymers or similar phenomena, as reported for PP-OH by Chung *et al*.[43]

D-E hysteresis behavior under high electric fields

Figure 5 compares the *D-E* loops obtained for pure PMP polymer and PMP ionomers film samples with different comonomer units and a thickness of ~10 μm after stretching measured at the same breakdown field. For each sample, a DC electric field was applied across the polymer film with initial amplitude of 100 MV/m, which was then increased gradually at intervals of 100 MV/m until reaching 600 MV/m. For the pure PMP polymer, a linear *D-E* loop with negligible hysteresis was observed, which indicates a constant dielectric constant of approx. 2.2 (calculated from the slope) and a completely reversible polarization-depolarization for the applied electric fields. Fortunately, for the PMP ionomers with different comonomer units, similar linear and slim loops were obtained, and the slope of the *D-E* loops was found to increase with the dielectric constant. For the PMP-$(NH_3)_3PO_4^{3-}$-4.5 polymers, the charge displacement could reach 0.027 C/m^2 at 600 MV/m, which is two times higher than the charge displacement observed for pure PMP at the same electric field.

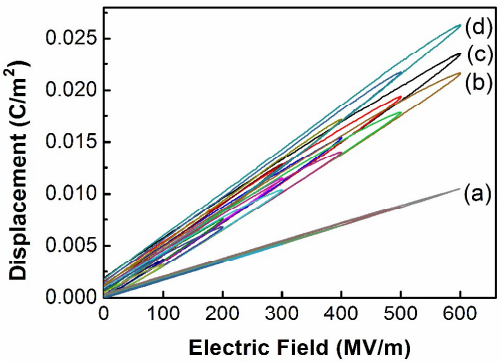

Fig. 5 *D-E* hysteresis loops obtained for different applied electric fields for (a) PMP and three different PMP-A-4.5 copolymers containing (b) Cl^-, (c) SO_4^{2-} and (d) PO_4^{3-} ions, respectively.

Most interestingly, the PMP-$(NH_3)_3PO_4^{3-}$-4.5 film sample showed a slimmer loop compared to the other ionomer films, indicating a lower hysteresis and faster polarization reversibility. When comparing with the PMP-$(NH_3)_2SO_4^{2-}$-4.5 film, the results obtained for both the dielectric constant (vs frequency and temperature) and the polarization loops (vs applied electric field) clearly indicate the unique contribution of the $(NH_3)_3PO_4^{3-}$ group to the properties of the PMP-$(NH_3)_3PO_4^{3-}$-4.5 dielectric thin film; the group not only increases the polarization but also provides a stable structure and morphology over a wide range of applied electric fields and at elevated temperatures. This PMP-$(NH_3)_3PO_4^{3-}$-4.5 film may exhibit a physical network structure which allows fast polarization-depolarization cycles with a limited hysteresis and a low energy loss.

The introduction of ionic functional groups into polymer chains usually results in a higher conduction loss under an applied electric field. Mechanical stretching is generally regarded as a common means to improve the mechanical properties, reduce the dielectric loss and enhance the breakdown strength of polymer films mainly based on the reduction of free volume during film stretching process. Fortunately, the mechanical stretching process may benefit from the increased melt viscosity caused by the addition of ionic groups to the polymer chains and the resulting formation of

View Article Online
DOI: 10.1039/C5TA09949H

physical cross-links. In case of PMP-$(NH_3)_3PO_4^{3-}$-4.5, the combination of the incorporation of ionic groups and a mechanical stretching process proved successful. The dielectric loss observed for PMP-$(NH_3)_3PO_4^{3-}$-4.5 continuously decreased as the stretching ratio was further increased even at higher electric fields, as illustrated in Figure 6.

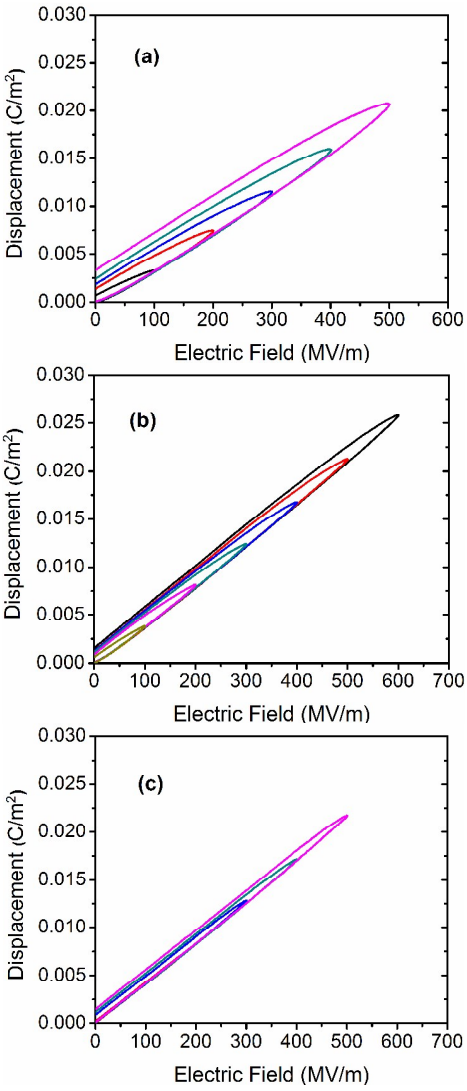

Fig. 6 Unipolar *D-E* loops obtained for the PMP-$(NH_3)_3PO_4^{3-}$-4.5 films: (a) after the hot pressing process (thickness: about 25 μm), (b) after uniaxial stretching to 250% of the original length (thickness: about 15 μm) and (c) after uniaxial stretching to 600% of the original length (thickness: about 9 μm).

Energy storage capability

The energy densities and charge-discharge energy efficiencies *η* calculated from the *D-E* loops are shown in Figure 7. The energy density clearly exponentially increases with the applied electric field. The PMP-$(NH_3)_3PO_4^{3-}$-4.5 ionomer shows a higher energy density under the same electric field than the other copolymers due to its higher dielectric constant and lower loss. The energy density obtained for the PMP-$(NH_3)_3PO_4^{3-}$-4.5 polymer film is 7.4 J/cm^3, which is more than twice the energy density observed for the pure PMP polymer and commercial BOPP capacitors, and also higher than values reported in literature for other polymer films.[43-48] Most importantly, the increase in energy density does not cause a significant increase in energy loss, which was calculated from the area enclosed by the charging-discharging cycle. The *η* calculated for the pure PMP polymer is around 97%, whereas the *η* calculated for the PMP-$(NH_3)_3PO_4^{3-}$-4.5 polymer film only decreased to 93% under an electric field of 600 MV/m, which indicates that the introduction of an ionic functional group can significantly improve the energy density while at the same time maintaining a high charge-discharge energy efficiency.

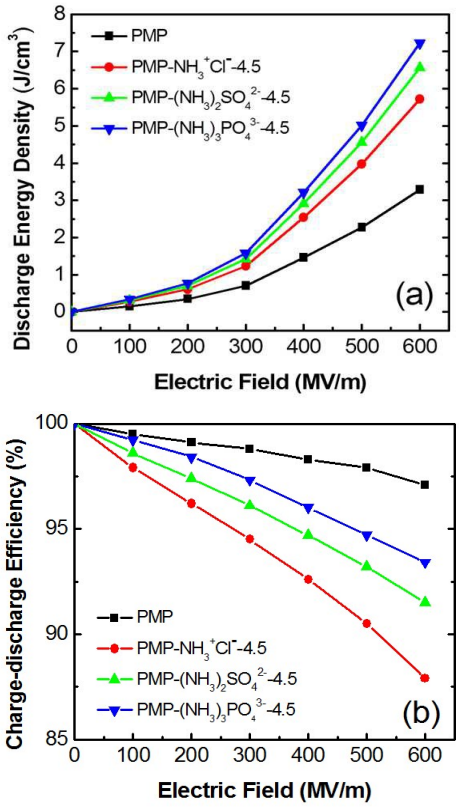

Fig. 7 (a) Energy density and (b) energy efficiency *η* of the PMP-$NH_3^+Cl^-$-4.5, PMP-$(NH_3)_2SO_4^{2-}$-4.5 and PMP-$(NH_3)_3PO_4^{3-}$-4.5 films compared with PMP (at 10Hz).

The four different types of polymer film, PMP, PMP-$NH_3^+Cl^-$-4.5, PMP-$(NH_3)_2SO_4^{2-}$-4.5 and PMP-$(NH_3)_3PO_4^{3-}$-4.5 were tested at different spots more than ten times, and the experimental results were fitted by a Weibull distribution function F(x),[52–54]

$$F(x) = 1 - e^{-(x/\alpha)^{\beta}} \quad (3)$$

where *α* is the scale parameter and refers to a 63.2% probability of failure [for x = α, F(x) = 0.632], and β denotes the shape parameter and describes the form of the distribution. Figure 8 shows the Weibull distributions with the estimated α and β values. Obviously,

View Article Online
DOI: 10.1039/C5TA09949H

the ionic cross-linking has a significant effect on the breakdown strength and the breakdown distribution – the higher the cross-linking density, the higher the breakdown strength (α), and the more narrow the distribution (β). The PMP-$(NH_3)_3PO_4^{3-}$-4.5 thin film, prepared by stretching after the hot pressing process, shows a breakdown strength between 540 and 660 MV/m with α = 612 MV/m, which is almost the same value obtained for BOPP films that are carefully conditioned (through stretching and annealing) to increase the chain orientation and crystallization and to reduce defects. In addition, the PMP-$(NH_3)_3PO_4^{3-}$-4.5 film exhibits a very narrow breakdown distribution with an exceptionally high β value of 34, indicating an excellent dielectric reliability – a very important quality in capacitor applications. The combination of a high dielectric constant (ε = 5.1), a relatively high breakdown strength (α = 612 MV/m), and a low energy loss in the PMP-$(NH_3)_3PO_4^{3-}$-4.5 dielectric film offers a reliable energy density of 7.4 J/cm^3, which is significantly higher than the energy density of 2–3 J/cm^3 typically obtained for BOPP capacitors.

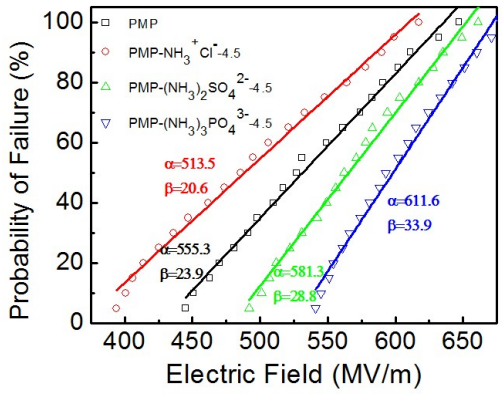

Fig. 8 Weibull plot comparing the experimental and theoretical dielectric breakdown strength for the four different types of polymers.

Conclusions

In conclusion, the dielectric performance and energy storage capacity of PMP polymer films can be significantly improved by ionic cross-linking. Compared to Cl^- and SO_4^{2-}, the PO_4^{3-} group with three negative charges can attract more positive charges in the polymer chains, which increase the viscosity of the polymer and leads to a more easy formation of the cross-linking network. The PMP-$(NH_3)_3PO_4^{3-}$-4.5 thin film, prepared by stretching after the hot pressing process, showed an enhanced dielectric constant (> 5) over a wide temperature range (–20 to 160 °C). The observed high energy density (7.4 J/cm^3) at a high breakdown strength (600 MV/m), the high charge-discharge energy efficiency (93%) and very narrow breakdown distribution (β = 34) are beneficial to the energy storage capabilities of future capacitor devices. The proposed synthesis method can serve as a general guideline for enhancing the dielectric properties and improving the application potential of polymer films for a future application in energy storage devices.

Acknowledgements

This work was supported by the National Natural Science Foundation of China (Grant Nos. 51532003 and 21404084), the Fundamental Research Funds for the Central Universities (Grant No. B040307), the State Key Laboratory of Solidification Processing in NWPU (Grand No. 107-QP-2014) and the 111 Project (Grant No. B08040).

References

1 T. Ōsaka, M. Datta, *Energy Storage Systems in Electronics*, CRC, Amsterdam, The Netherlands 2000.
2 H. S. Nalwa, *Handbook of Low and High Dielectric Constant Materials and Their Applications. Volume 1: Materials and Processing. Volume 2: Phenomena, Properties and Applications*, Academic Press, New York, 1999.
3 M. Rabuffi, G. Picci, *IEEE Trans. Plasma Sci.* 2002, **30**, 1939.
4 B. Chu, X. Zhou, K. Ren, B. Neese, M. Lin, Q. Wang, F. Bauer, Q. M. Zhang, *Science* 2006 , **313**, 334.
5 P. Kim, N. M. Doss, J. P. Tillotson, P. J. Hotchkiss, M.-J. Pan, S. R. Marder, J. Li, J. P. Calame, J. W. Perry, *ACS Nano* 2009, **3**, 2581.
6 Z. M. Dang, J. K. Yuan, J. W. Zha, T. Zhou, S. T. Li, G. H. Hu, *Prog. Mater. Sci.* 2012, **57**, 660.
7 Q. Wang and L. Zhu, *Macromolecules* 2012, **45**, 2937.
8 Q. Li, L. Chen, M. R. Gadinski, S. Zhang, G. Zhang, H. Li, A. Haque, L. Q. Chen, T. Jackson, Q. Wang, *Nature* 523, 576 (2015).
9 Q. Wang and L. Zhu, *J. Polym. Sci. Part B Polym. Phys.* 2011, **49**, 1421.
10 L. Zhang and Z.-Y. Cheng, *J. Adv. Dielectr.* 2011, **1**, 389.
11 Z. M. Dang, J. K. Yuan, S. H. Yao, R. J. Liao, *Adv. Mater.*2013, **25**, 6334.
12 Y. Cao, P. C. Irwin, K. Younsi, *IEEE Trans. Dielect. Elect. Insul.* 2004, **11**, 797.
13 L. A. Fredin, Z. Li, M. A. Ratner, M. T. Lanagan, T. J. Marks, *Adv. Mater.* 2012, **24**, 5946.
14 J. H. Tortai, N. Bonifaci, A. Denat, *J. Appl. Phys.* 2005, **97**, 053304.
15 Q. Tan, P. Irwin, Y. Cao, *IEEJ Trans. Fund. Mater.* 2006, **126**, 1152.
16 G. Picci, M. Rabuffi, *IEEE Trans. Plasma Sci.* 2000, **28**, 1603.
17 Z. C. Zhang, T. C. Chung, *Macromolecules*, 2007, **40**, 783.
18 Z. C. Zhang, T. C. Chung, *Macromolecules*, 2007, **40**, 9391.
19 T. C. Chung, A. Petchsuk, U.S. Patent 6,355,749.
20 A. Lovinger, *Science* 1983, **220**, 1115.
21 J. Claude, Y. Lu, Q. Wang, *Appl. Phys. Lett.* 2007, **91**, 212904.
22 X. Zhou, B. J. Chu, B. Neese, M. R. Lin, Q. M. Zhang, *IEEE Trans. Dielectr. Electr. Insul.* 2007, **14**, 1133.
23 J. Claude, Y. Lu, K. Li, Q. Wang, *Chem. Mater.* 2008, **20**, 2078.
24 X. Zhou, X. Zhao, Z. Suo, C. Zou, J. Runt, S. Liu, S. Zhang, Q. M. Zhang, *Appl. Phys. Lett.* 2009, **94**, 162901.
25 F. X. Guan, J. L. Pan, J. Wang, Q. Wang, L. Zhu, *Macromolecules* 2010, **43**, 384.
26 M. Rahimabady, K. Yao, S. Arabnejad, L. Lu, V. P. W. Shim, D. C. W. Chet, *Appl. Phys. Lett.* 2012, **100**, 252907.
27 V. K. Thakur, E. J. Tan, M. F. Lin, P. S. Lee, *J. Mater. Chem.* 2011, **21**, 3751.
28 V. K. Thakur, E. J. Tan, M. F. Lin, P. S. Lee, *Polym. Chem.* 2011, **2**, 2000.
29 V. K. Thakur, E. J. Tan, M. F. Lin, P. S. Lee, *J. Mater. Chem.* 2012, **22**, 5951.
30 K. Tashiro, *Crystal structure and phase transition of PVDF and related copolymers. in Ferroelectric Polymers: Chemistry,*

View Article Online
DOI: 10.1039/C5TA09949H

Physics, and Applications. (ed Nalwa, H. S.) 63–182 1st Ed. (Dekker, 1995).
31 Y. Lu, J. Claude, B. Neese, Q. M. Zhang, Q. Wang, *J. Am. Chem. Soc.* 2006, **128**, 8120.
32 T. Furukawa, M. Date, E. Fukada, *J. Appl. Phys.* 1980, **51**, 1135.
33 T. Furukawa, *Phase Trans.* 1989, **18**, 143.
34 V. Ranjan, L. Yu, M. B. Nardelli, J. Bernholc, *Phys. Rev. Lett.* 2007, **99**, 047801.
35 F. X. Guan, Z. Yuan, E. W. Shu, L. Zhu, *Appl. Phys. Lett.* 2009, **94**, 052907.
36 F. X. Guan, J. Wang, L. Y. Yang, J. K. Tseng, K. Han, Q. Wang, L. Zhu, *Macromolecules* 2011, **44**, 2190.
37 F. X. Guan, L. Y. Yang, J. Wang, B. Guan, K. Han, Q. Wang, L. Zhu, *Adv. Funct. Mater.* 2011, **21**, 3176.
38 J. J. Li, S. B. Tan, S. J. Ding, H. Y. Li, L. J. Yang, Z. C. Zhang, *J. Mater. Chem.* 2012, **22**, 23468.
39 J. J. Li, X. Hu, G. X. Gao, S. J. Ding, H. Y. Li, L. J. Yang, Z. C. Zhang, *J. Mater. Chem. C.* 2013, **1**, 1111.
40 P. Khanchaitit, K. Han, M. R. Gadinskl, Q. Li, Q. Wang, *Nature Communication.* 2013, 1.
41 J. Pan, K. Li, J. Li, T. Hsu, Q. Wang, *Appl. Phys. Lett.* 2009, **95**, 022902.
42 J. Pan, K. Li, S. Chuayprakong, T. Hsu, Q. Wang, *Applied Materials & Interfaces*. 2010, **2**, 1286.
43 X. Yuan, Y. Matsuyama, T. C. Mike Chung, *Macromolecules* 2010, **43**, 4011.
44 M. Misra, M. Agarwal, D. W. Sinkovits, S. K. Kumar, C. C. Wang, G. Pilania, R. Ramprasad, R. A. Weiss, X. P. Yuan, T. C. M. Chung, *Macromolecules* 2014, **47**, 1122.
45 S. Wu, W. Li, M. Lin, Q. Burlinggame, Q. Chen, A. Payzant, K. Xiao, Q. M. Zhang, *Adv. Mater.* 2013, **25**, 1734.
46 Q. Burlinggame, S. Wu, M. Lin, Q. M. Zhang, *Adv. Energy. Mater.* 2013, **3**, 1051.
47 M. Zhang, X. Yuan, L. Wang, T. C. Mike Chung, *Macromolecules* 2014, **47**, 571.
48 M. Zhang, H. K. Kim, E. Chalkova, F. Mark, S. N. Lvov, T. C. Mike Chung, *Macromolecules* 2011, **44**, 5937.
49 L. Xie, X. Huang, K. Yang, S. Li, P. Jiang, *J. Mater. Chem. A*, 2014, **2**, 5244.
50 L. Ren, X. Meng, J.-W. Zha, Z. M. Dang, *RSC Adv.*, 2015, **5**, 65167.
51 J. Yuan, A. Luna, W. Neri, C. Zakri, T. Schilling, A. Colin, P. Poulin, *Nature Comm.* 2015, **6**, 8700.
52 W. Weibull, *ASME Trans. J. Appl. Mech.* 1951, **18**, 293.
53 J. C. Fothergill, *IEEE Trans. Electr. Insul.* 1990, **25**, 489.
54 H. Goshima, N. Hayakawa, M. Hikita, H. Okubo, K. Uchida, *IEEE Trans. Dielectr. Electr. Insul.* 1995, **2**, 385.